RESEARCH ARTICLE

High Precision and Large Dynamic Range Measurement of Laser Triangulation Displacement Sensor Using Diffraction Grating

YANRONG YANG[1,5,6], **XUEHUA CHEN**[2], **LINHAI HUANG**[3,4], **NAITING GU**[3,4], **YAWEI XIAO**[3,4], **AND HAO CHEN**[3,4]

[1]College of Ophthalmology, Chengdu University of Traditional Chinese Medicine, Chengdu 610075, China
[2]Beijing Academy of Quantum Information Sciences, Beijing 100193, China
[3]Key Laboratory of Adaptive Optics, Chinese Academy of Sciences, Chengdu 610209, China
[4]University of Chinese Academy of Sciences, Beijing 100029, China
[5]Key Laboratory of Sichuan Province Ophthalmopathy Prevention and Cure and Visual Function Protection with Traditional Chinese Medicine, Chengdu 610075, China
[6]Ineye Hospital, Chengdu University of Traditional Chinese Medicine, Chengdu 610075, China

Corresponding author: Hao Chen (chenhao114@mails.ac.cn)

ABSTRACT The conventional laser triangulation displacement sensor (LTDS) is difficult to achieve large dynamic range and high precision measurement simultaneously, since LTDS is affected by factors such as limited detector size, nonlinear input and output variables, laser power fluctuation, speckle noise, electronic noise, etc. Given the above background, we proposed a modified LTDS using a diffraction grating to improve the dynamic range and precision simultaneously. Different from the conventional LTDS, the modified LTDS generates more than one spots on the image sensor, thereby the displacements with different ranges can be obtained from the multiple order diffraction spots. Ultimately, the dynamic range and measurement accuracy will be improved simultaneously by integrating these displacements. In this paper, the principle of the modified LTDS for large dynamic range and high precision measurement is described in detail, and we verified the validity and effectiveness of this idea through the experiment. Compared with the traditional LTDS, the experimental results show that the linearity of the modified LTDS is improved by a factor of 1.5685 and the dynamic range is improved 1.2986 times as well as maintaining the same linearity.

INDEX TERMS Laser triangulation displacement sensor, diffraction grating, large dynamic range, high precision.

I. INTRODUCTION

Laser triangulation displacement sensor (LTDS) is one of the most commonly displacement sensors as it is non-contact, presents high precision, good robustness and cost effectiveness [1], [2], [3]. According to the geometry relationship between the source, the object and the position-sensitive detector, the object displacement can be determined from the

The associate editor coordinating the review of this manuscript and approving it for publication was Zeev Zalevsky.

spot image at the sensor. In recent years, LTDS has been widely used in many branches, such as precision engineering [4], [5], [6], aerospace manufacturing [7], equipment condition monitoring [8], materials science [9], traditional Chinese medicine science [10], [11] and agricultural science [12], [13]. Researchers have done a lot of work on improving the performance of LTDS, such as increasing the freedom degree, enhancing the range, and expanding the measurable material types. Zeng et al. [14] demonstrated a two-beam LTDS for measuring the displacement of a moving object

in both longitudinal and transverse directions. Liu et al. [15] proposed a diffraction-type LTDS by mounting a reflective diffraction grating on the moving object. This configuration enables to measure the longitudinal displacement and additional three-rotation angular displacement of the moving object simultaneously. In [16], a LTDS with six image sensors was developed to simultaneously measure the distance and inclination angle of a work piece surface. In [17], a LTDS with enhanced range and resolution was developed through adaptive electronic control of the beam propagation parameters. In [18], a LTDS that utilizes a high-quality ultraviolet laser beam was developed for precise displacement measurement of object surface with diffuse, transparent, translucent, and others material types.

Despite various improvements that have been achieved, the measurement accuracy and range of longitudinal displacement are the core indicators for evaluating LTDS performance. The measurement precision can be affected by the factors such as the non-linearity between the input and output variables, laser power fluctuations, speckle noise, electronic noises and the surface orientation [19]. The measurement errors caused by the influential factors mentioned above have been widely investigated [20], [21], [22], [23], and some optimization methods have been proposed. In Refs. [24], [25], [26], several calibration methods have been proposed for effectively compensating the non-linearity of the triangulation measurement model. From the viewpoint of the improvement of signal processing, image segmentation [27] and digital speckle correlation methods [28] were proposed for improving the measurement precision. In 2021, Ye.et. al. [29] developed a LTDS with a grating placed after the imaging lens to improve the measurement accuracy. The result shown that the measurement nonlinearity and repeatability of the developed LTDS are 0.113% of full-scale (F.S. = 20 mm) and 0.89 μm respectively. Such the small full-scale is attributed to the small field of the imaging lens. In addition, the most important limiting factor is that the zero-order spot should be always on the sensor during the measuring. So far, there is no effective method to achieve the high precision and large dynamic range simultaneously. Generally, the dynamic range is mainly limited by the size of the sensor. From the viewpoint of the improvement of sensor configuration, a LTDS that consists of three CCD distributed uniformly along the optical axis was designed in Ref. [30]. At present, only this configuration enables higher precision by measuring the large-size displacement in sections.

In this paper, a modified LTDS configuration with the diffraction grating placed in front of the imaging lens is proposed, which is different from the structure in 29. We introduce a new principle of the modified LTDS. Based on the principle, a high precision and large dynamic range will be achieved as the zero-order diffraction spot can be absent on the sensor when measuring. Each spot can be used to measure the displacements with different ranges. Thus, the dynamic range will be increased when combining the different order spots, and measurement accuracy will be improved
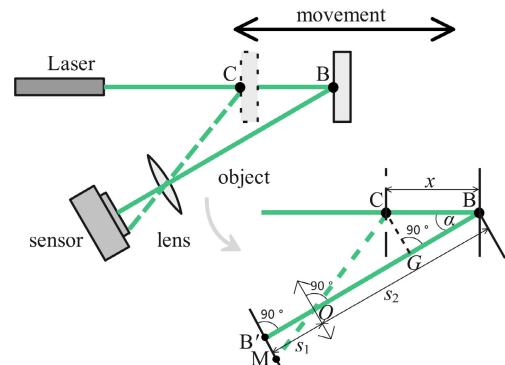

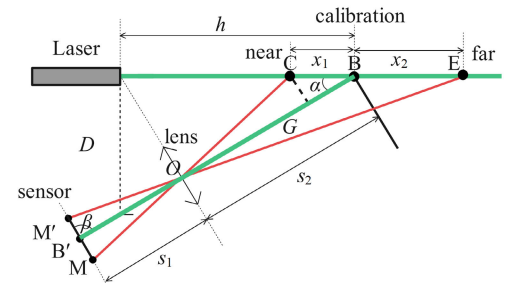**FIGURE 1.** Measurement principle of a typical vertical-incidence conventional LTDS.

FIGURE 2. Schematic diagram of conventional LTDS measurement range. h, working distance. D, baseline.

by averaging. The validity and effectiveness of the modified LTDS have been confirmed from experimental results.

II. PRINCIPLE AND METHOD
A. MEASUREMENT PRINCIPLE OF A CONVENTIONAL LTDS
The measurement principle of a conventional LTDS is shown in Fig.1. The laser light incidents on the object surface, and the diffuse reflection is projected on the sensor of a high-resolution CMOS (Complementary Metal Oxide Semiconductor) by the imaging lens. As the optical structure does not meet the Scheimpflug condition, the random displacement x can be derived as follows.

Taken B as the calibration point, and B$'$ is the image point on the sensor. When the object moving to C, the corresponding image is M. The displacement x can be derived from the similarity between $\triangle OCG$ and $\triangle OMB'$.

$$\frac{s_1 \sin\alpha}{B'M} = \frac{s_2 - x\cos\alpha}{s_1}. \tag{1}$$

Thus,

$$x = \frac{s_2 B'M}{s_1 \sin\alpha + B'M \cos\alpha} \tag{2}$$

s_2 and s_1 are the object distance and image distance in the imaging of B, respectively. α is the working angle between the incident light and BB'. The measurement range of the conventional LTDS can be determined by the system parameters, as shown in Fig. 2. The point M and M$'$ are the edge of the sensor. Thus, the measurement distance will be ranging from the near point C to the far point E.

x_1 is the length of BC, x_2 is the length of BE. M and M$'$ are the images of C and E. β is the angle between the sensor and

BB'. As we know that the β is set to 90° in Eq. (1). But in the actual applications, it is difficult to make β to meet the right angle. Thus, different from the Eq. (1), x_1 can be re-derived from the Law of Sines in the ΔOCB, as

$$x_1 = \frac{s_2 \sin \angle BOC}{\sin (\alpha + \angle BOC)}. \quad (3)$$

In ΔOEB, the following formula is obtained based on the Law of Sines,

$$x_2 = \frac{s_2 \sin \angle BOE}{\sin (\alpha - \angle BOE)}. \quad (4)$$

The angle $\angle BOE$ and $\angle BOC$ can be presented as,

$$\begin{cases} OM' = s_1^2 + B'M'^2 - 2s_1 \times B'M' \times \cos(\beta) \\ OM = s_1^2 + B'M^2 - 2s_1 \times B'M \times \cos(180 - \beta) \\ \angle BOE = \angle B'OM' = \arccos\left(\frac{s_1^2 + OM'^2 - B'M'^2}{2s_1 \times OM'}\right) \\ \angle BOC = \angle B'OM = \arccos\left(\frac{s_1^2 + OM^2 - B'M^2}{2s_1 \times OM}\right) \end{cases} \quad (5)$$

where the distances of $B'M$ and $B'M'$ can be calculated from the sensor images. The measurement range of conventional LTDS can be presented as,

$$L = x_1 + x_2 = \frac{s_2 \sin \angle BOC}{\sin (\alpha + \angle BOC)} + \frac{s_2 \sin \angle BOE}{\sin (\alpha - \angle BOE)}. \quad (6)$$

B. MEASUREMENT PRINCIPLE OF THE MODIFIED LTDS

The measurement principle of the modified LTDS with a diffraction grating is shown in Fig.3. Different from the conventional configuration presented in Fig. 1, the diffraction grating is located in front of the imaging lens. Thus, multiple diffraction spots such as 0th, −1th, and +1th orders etc. will be imaged on the sensor during a single capture and the displacement can be measured by any of the distinguishable spots on the sensor. Then, the displacements with different ranges can be obtained from different order diffraction spots. Fig. 3 shows the geometric relationship between the position of multiple order spots and the displacements of the object. It can be seen that the propagation path of the 0th spot is consistent with that of the conventional LTDS.

In Fig.3, B is the calibrated point, C is a random point of the object. The lens is parallel to the sensor. A_0 and A_m are 0th and negative mth order images of B on the sensor, respectively. Similarly, A_0' and A_m' are the 0th and negative mth order images of C. φ_m and φ_m' are the negative mth order diffraction angle of the point B and C. d_m is the distance of A_0A_m', which can be calculated from the diffraction images. In $\Delta A_0QA_m'$, $\angle A_0QA_m'$ can be presented as,

$$\angle A_0QA_m' = \arccos \frac{QA_0^2 + QA_m'^2 - d_m^2}{2QA_0 \times QA_m'} \quad (7)$$

where, $QA_0 = s_1 + s_3$, s_3 is the distance between the grating and lens. QA_m' can be calculated as,

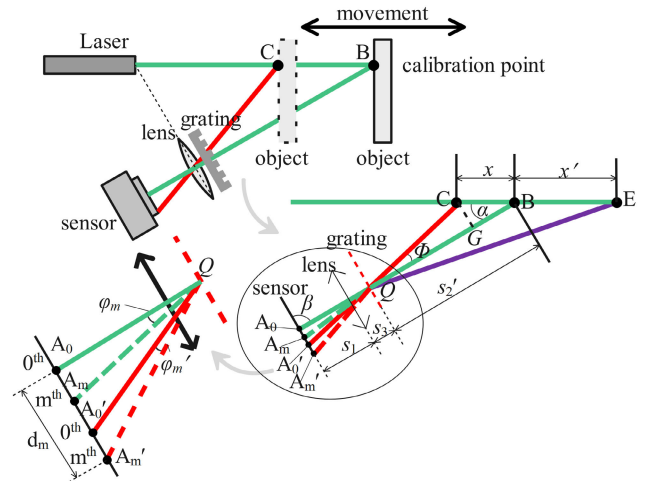$$QA_m' = d_m^2 + QA_0^2 - 2 \times d_m \times QA_0 \times \cos(180 - \beta). \quad (8)$$

FIGURE 3. Measurement principle of the modified LTDS.

From the negative m-th order spot A_m', we can calculate the incident angle $\angle BQC$ base on the diffraction equation of grating,

$$\angle BQC = \Phi = \arcsin\left(-\frac{m\lambda}{p} + \sin(\angle A_0QA_m')\right). \quad (9)$$

Then, the distance of x can be obtained by Eq. (3), as

$$x = \frac{s_2' \sin \angle BQC}{\sin (\alpha + \angle BQC)}, \quad (10)$$

where s_2' is the vertical distance from B to the grating. Thus, as long as d_m is measured, the distance of x will be calculated. It means that each order spot can be used to calculate the displacement no matter the zero-order diffraction spot is appeared or absent on the sensor. Similarly, the x' in Fig.3 can be calculated as

$$x' = \frac{s_2' \sin \angle BQE}{\sin (\alpha - \angle BQE)}. \quad (11)$$

Thus, using the distance of d_m, the modified LTDS can measure the displacements x and x'. Through averaging the displacements calculated from the spots, a higher measurement precision can be achieved.

The measurement range of the modified LTDS is shown in Fig. 4. Again, B is the calibration point, M and M' are the edge of the sensor. The measuring distance of the conventional LTDS is ranging from the point C to B. Different from the conventional LTDS, when the modified LTDS measures the object at the near point T, the 0th order diffraction spot N is falling outside the sensor, but the positive m-th order spot M just within the sensor. So, the modified LTDS can measure the displacement of BT through the m-th order spot. Similarly, when the object at the far point F, the 0th order diffraction spot N' is falling outside the sensor, but the negative m-th order spot M' is just can be used to measure the displacement of BF.

Thus, the distances of L_1 and L_2 are the increasing parts. L_1 and L_2 can be calculated through Eqs. (10) and (11). The
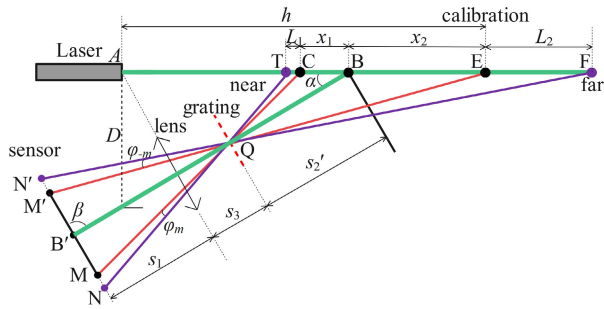
FIGURE 4. Schematic diagram of LTDS with diffraction grating. h, working distance. D, baseline.

dynamic range of the modified LTDS can be presented as,

$$L = L_1 + L_2 + x_1 + x_2. \qquad (12)$$

In order to evaluate the improvement, the corresponding evaluation indicators are given here, as the dynamic range magnification factor ρ and the linearity δ. ρ and δ defined as,

$$\rho = \frac{L_1 + L_2 + x_1 + x_2}{x_1 + x_2}, \qquad (13)$$

$$\delta = \frac{\Delta x_{\max}}{L} \times 100\%, \qquad (14)$$

where Δx_{max} is the maximum measurement error.

III. EXPERIMENT AND RESULTS

In the experiment, the diffraction grating is placed close to the front of the imaging lens, as shown in Fig. 5. The commercial large-field imaging lens is used to achieve a larger dynamic range and the threaded connector can ensure that the lens parallel to the sensor. The wavelength of the semiconductor laser (DD532-50-5, Xi'an Huake Optoelectronics Co., Ltd, China) is 532 nm. The CMOS size is 7.4 mm (Basler, acA4042-29um), and the grating constant p is 33 lines / mm. The working distance h is 419 mm, the baseline D is 373 mm, the focal length f of the lens is 12 mm. The object, which is a cardboard box, is moved by the computer-controlled translation platform (CL-01A, Haijie Technology, China) in 2.5 mm every step, the image of each step will be used to calculate the displacement. Simultaneously, the actual displacements were measured by a grating ruler (ranging from 50 mm to 1000 mm with the precision 1 μm), as the actual position. In order to remove the background noise from surrounding objects diffused reflections, a narrowband filter at 532 nm was used in the experiment.

The intensity distribution of multiple order spots is shown in Fig. 6. Fig. 6 (b) is sum of the intensities between the two red lines in Fig. 6 (a) along the image height. The spot orders can be determined according to the intensity. As the grating is a transmission phase diffraction, the energy of the 0th order is less than ±1th order, marked with the black circle in Fig. 6(a). The positive and negative order spots are separated on both sides of the 0th order spot. Starting from the farthest point, the first spots appeared on the sensor is the negative order. The negative order ($\leq$-2) diffraction spots
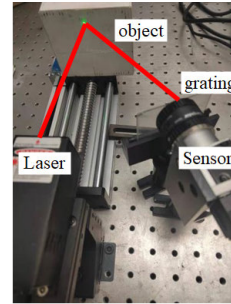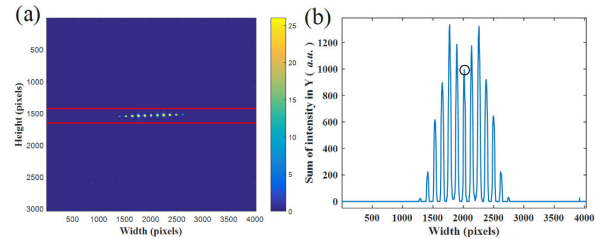

FIGURE 5. Experimental device.

FIGURE 6. The spots image of the sensor (a) and its intensity distribution (b).
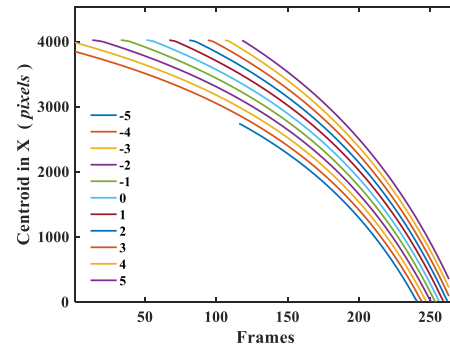

FIGURE 7. The centroids of spots along image width.

conform to the rule that the intensity of negative m-th order spot is larger than the previous order and lower than the last order. On the contrary, the intensity of positive ($\geq$2) m-th order spot is lower than the previous order and larger than the last order. As the object moves closer, the diffraction spots will gradually be appeared on the sensor, as -5th, -4th, -3th, -2th, -1th, 0th, 1th and other positive orders. According to the experimental parameters, the sensor can obtain the spots up to eleven, as shown in Fig. (6). The other spots or dots intensities are too weak to be used in measurement.

Figure 6 is captured at the calibrating point. As the spot orders can be determined in advance, we take the intensity distribution in Fig. 6(b) as the reference. Then, calculate the cross-correlation between the intensity distributions in other images and the reference. Based on the cross-correlation, the spot orders of each image, which should have at least two actual incident spots, can be determined with real-time. The coordinates of each spot can be calculated by the centroid of the spots, as shown in Fig. (7). The sensor captured 263 frames of images. The first image corresponding to the farthest distance, there only -4th and -3th order diffraction spots can be identified. The -5th order spots were not identi-
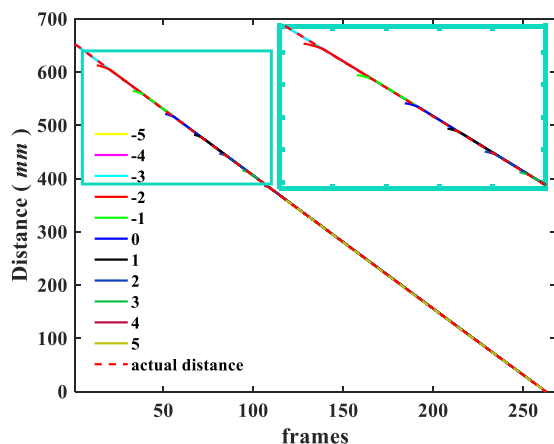
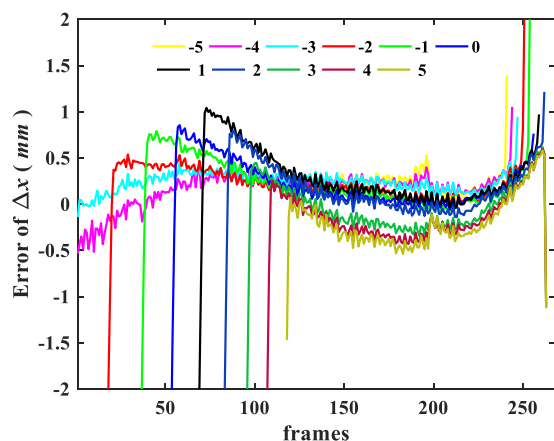**FIGURE 8.** The distances measured from each order spots.

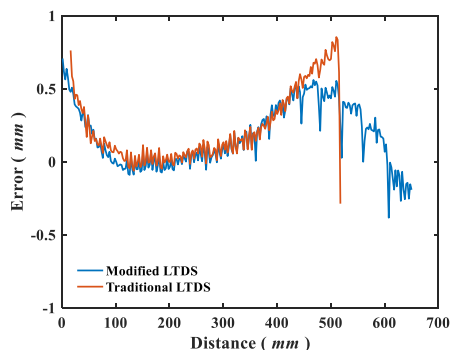**FIGURE 9.** The errors corresponding to each order spots.

FIGURE 10. Measurement range and error calculated by multiple orders and 0th order.

fied in the initial frames as the weakly intensities, which only can be measured from 116 to 241 frames. Except the -5th spot, the other order spots were gradually appeared on the sensor when the object moved from a far to a near position. Besides, all the spots would be gradually disappeared on the sensor.

The distance curves calculated through these order spots are basically coincidence with the actual distance measured by the grating ruler, as shown in Fig. 8.

Compared to the actual distance, the measurement errors are shown in Fig. 9. Removing the abnormal values at endpoints, the mean error is 0.1480 ± 0.2631 mm

TABLE 1. Measurement range, maximum error and linearity of each order.

Order spots	Measurement range(mm)^a	Maximum error(mm)	F.S. ^{b} (%)
+5	1.2123~367.9908	0.5819	0.1587
+4	1.2123~385.4421	0.7135	0.1857
+3	1.2123~412.8676	0.6170	0.1499
+2	3.6493~445.3697	0.9701	0.2196
+1	8.6204~480.3070	1.0423	0.2210
-1	23.6029~560.3106	0.7903	0.1472
-2	31.0588~605.3229	0.8102	0.1411
-3	38.5534~652.8010	0.9446	0.1538
-4	53.5359~652.8010	0.5369	0.0896
-5	56.0427~365.4553	0.5273	0.1704
0	16.1184~517.8689	0.8554	0.1705

^{a} The zero of the grating ruler is set as the measuring origin.

^{b} F.S., full scale.

(mean± variance, ranging from -1.0943 to 1.0534 mm). The detailed values of measurement ranges, maximum errors and the linearity δ of the modified LTDS under each order are shown in Table 1.

Using the multiple order spots, a large dynamic measuring range will be achieved, as shown in Fig.10. Also, the modified LTDS can combine the multiple orders to reduce the random errors of the system and improve the measurement precision. While the range of the traditional LTDS is equal to the range of 0th order spot.

The measurement range of 0th spot is 501.7505 mm which ranged from 16.1184 to 517.8689 mm, the maximum error is 0.8554 mm and δ is 0.1705%, as shown in Fig.10 (blue line). While using the multiple order spots, the measurement range of the modified LTDS is 651.5887 mm which ranged from 1.2123 to 652.8010 mm, the maximum error is 0.7085 mm and δ is 0.1087%. Thus, the modified LTDS improved the measurement range by 1.2986 times and the linearity δ by a factor 1.5685.

IV. CONCLUSION

In summary, we have presented a modified LTDS configuration, in which a diffraction grating was placed in front of the imaging lens. Compared to the conventional LTDS, the modified LTDS can measure the displacements with different ranges from the multiple order spots. Then, combined these displacements to improve the dynamic range and measurement accuracy simultaneously. The validity and effectiveness of the modified LTDS has been confirmed from the experimental results. That may give us some inspiration for long-distance and high-precision measurement and 3D reconstruction of super large objects.

REFERENCES

[1] Y. Li, M. Kästner, and E. Reithmeier, "Triangulation-based edge measurement using polyview optics," *Opt. Lasers Eng.*, vol. 103, pp. 71–76, Apr. 2018.

[2] J. P. Makai, "Simultaneous spatial and angular positioning of plane specular samples by a novel double beam triangulation probe with full auto-compensation," *Opt. Laser Eng.*, vol. 77, pp. 42–137, Feb. 2016.

[3] W. Chen, Z. Ni, X. Hu, and X. Lu, "Research on pavement roughness based on the laser triangulation," *Photonic Sensors*, vol. 6, no. 2, pp. 177–180, Mar. 2016.

[4] H.-L. Huang, W.-Y. Jywe, C.-H. Liu, L. Duan, and M.-S. Wang, "Development of a novel laser-based measuring system for the thread profile of ballscrew," *Opt. Lasers Eng.*, vol. 48, no. 10, pp. 1012–1018, 2010.

[5] D. Bračun, V. Gruden, and J. Možina, "A method for surface quality assessment of die-castings based on laser triangulation," *Meas. Sci. Technol.*, vol. 19, no. 4, Mar. 2008, Art. no. 045707.

[6] S. Paulus, T. Eichert, H. Goldbach, and H. Kuhlmann, "Limits of active laser triangulation as an instrument for high precision plant imaging," *Sensors*, vol. 14, no. 2, pp. 2489–2509, Feb. 2014.

[7] B. Sun and B. Li, "Laser displacement sensor in the application of aero-engine blade measurement," *IEEE Sensors J.*, vol. 16, no. 5, pp. 1377–1384, Mar. 2016.

[8] A. Maekawa, M. Noda, and M. Shintani, "Experimental study on a non-contact method using laser displacement sensors to measure vibration stress in piping systems," *Measurement*, vol. 79, pp. 101–111, Feb. 2016.

[9] H. Liu, D. Niu, W. Jiang, T. Zhao, B. Lei, L. Yin, Y. Shi, B. Chen, and B. Lu, "Illumination-oriented and thickness-dependent photomechanical bilayer actuators realized by graphene-nanoplatelets," *Sens. Actuators A, Phys.*, vol. 239, pp. 45–53, Mar. 2016.

[10] J. H. Wu, W. L. Lee, Y. P. Lee, C. H. Lin, J. Y. Chiou, C. F. Tai, and J. A. Jiang, "An improved arterial pulsation measurement system based on optical triangulation and its application in the traditional Chinese medicine," in *Proc. SPIE*, Sep. 2011, Art. no. 81330U, doi: 10.1117/12.892959.

[11] J. H. Wu, R. S. Chang, and J. A. Jiang, "A novel pulse measurement system by using laser triangulation and a CMOS image sensor," *Sensors*, vol. 7, no. 12, pp. 3366–3385, Dec. 2007.

[12] D. Ehlert, H.-J. Horn, and R. Adamek, "Measuring crop biomass density by laser triangulation," *Comput. Electron. Agricult.*, vol. 61, no. 2, pp. 117–125, 2008.

[13] K.-C. Lee, J.-S. Yang, and H. H. Yu, "Development and evaluation of a petal thickness measuring device based on the dual laser triangulation method," *Comput. Electron. Agricult.*, vol. 99, pp. 85–92, Nov. 2013.

[14] L. Zeng, F. Yuan, D. Song, and R. Zhang, "A two-beam laser triangulation for measuring the position of a moving object," *Opt. Lasers Eng.*, vol. 31, no. 6, pp. 445–453, Jun. 1999.

[15] C. H. Liu, W. Y. Jywe, and C. K. Chen, "Development of a diffraction-type optical triangulation sensor," *Appl. Opt.*, vol. 43, no. 30, pp. 5607–5613. Oct. 2004.

[16] F.-J. Shiou and M.-X. Liu, "Development of a novel scattered triangulation laser probe with six linear charge-coupled devices (CCDs)," *Opt. Lasers Eng.*, vol. 47, no. 1, pp. 7–18, Jan. 2009.

[17] S. A. Reza, T. S. Khwaja, M. A. Mazhar, H. K. Niazi, and R. Nawab, "Improved laser-based triangulation sensor with enhanced range and resolution through adaptive optics-based active beam control," *Appl. Opt.*, vol. 56, no. 21, pp. 5996–6006, Jan. 2017.

[18] K. Žbontar, M. Mihelj, B. Podobnik, F. Povše, and M. Munih, "Dynamic symmetrical pattern projection based laser triangulation sensor for precise surface position measurement of various material types," *Appl. Opt.*, vol. 52, no. 12, pp. 2750–2760, Apr. 2013.

[19] B. Muralikrishnan, W. Ren, D. Everett, E. Stanfield, and T. Doiron, "Performance evaluation experiments on a laser spot triangulation probe," *Measurement*, vol. 45, no. 3, pp. 43–333, Apr. 2012.

[20] N. Vukašinović, D. Bračun, J. Možina, and J. Duhovnik, "The influence of incident angle, object colour and distance on CNC laser scanning," *Int. J. Adv. Manuf. Technol.*, vol. 50, no. 1, pp. 265–274, 2010.

[21] N. Van Gestel, S. Cuypers, P. Bleys, and J.-P. Kruth, "A performance evaluation test for laser line scanners on CMMs," *Opt. Laser Eng.*, vol. 47, nos. 3–4, pp. 336–342, 2009.

[22] J. Liu, L. Tian, and L. Li, "Light power density distribution of image spot of laser triangulation measuring," *Opt. Lasers Eng.*, vol. 29, no. 6, pp. 457–463, Jun. 1998.

[23] C. Dong, "A regression model for analysing the non-linearity of laser triangulation probes," *Int. J. Adv. Manuf. Technol.*, vol. 59, nos. 5–8, pp. 691–695, Mar. 2012.

[24] W. M. Ren, P. M. Sun, Y. L. Wang, and H. Zhu, "A calibration method for laser displacement system based on triangulation," *Opt. Technol.*, vol. 3, pp. 11–15, May 1997.

[25] J. Sun, J. Zhang, Z. Liu, and G. Zhang, "A vision measurement model of laser displacement sensor and its calibration method," *Opt. Lasers Eng.*, vol. 51, no. 12, pp. 1344–1352, Dec. 2013.

[26] J. Zhang, J. Sun, Z. Liu, and G. Zhang, "A flexible calibration method for laser displacement sensors based on a stereo-target," *Meas. Sci. Technol.*, vol. 25, no. 10, Sep. 2014, Art. no. 105103.

[27] T. Mueller and E. Reithmeier, "Image segmentation for laser triangulation based on Chan–Vese model," *Measurement*, vol. 63, pp. 100–109, Mar. 2015.

[28] L. Shen, D. Li, and F. Luo, "A study on laser speckle correlation method applied in triangulation displacement measurement," *Optik*, vol. 124, no. 20, pp. 4544–4548, Oct. 2013.

[29] G. Ye, Y. Zhang, W. Jiang, S. Liu, L. Qiu, X. Fan, H. Xing, P. Wei, B. Lu, and H. Liu, "Improving measurement accuracy of laser triangulation sensor via integrating a diffraction grating," *Opt. Lasers Eng.*, vol. 143, Aug. 2021, Art. no. 106631.

[30] X.-B. Fu, B. Liu, and Y.-C. Zhang, "A displacement measurement system based on optical triangulation method," *Optoelectron. Lett.*, vol. 7, no. 5, pp. 380–383, Oct. 2011.
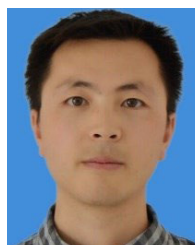
YANRONG YANG received the Ph.D. degree in optical engineering, in 2018. From 2018 to 2022, he was a Postdoctoral Student with the College of Ophthalmology, Chengdu University of Traditional Chinese Medicine. His current research interests include adaptive optics and human eye aberration measurement and correction.

XUEHUA CHEN, photograph and biography not available at the time of publication.

LINHAI HUANG, photograph and biography not available at the time of publication.

NAITING GU, photograph and biography not available at the time of publication.

YAWEI XIAO, photograph and biography not available at the time of publication.

HAO CHEN received the Ph.D. degree in optical engineering from the University of Chinese Academy of Sciences, Beijing, China, in 2020. Since 2020, he has been a Postdoctoral Researcher with the Key laboratory of Adaptive Optics, Chinese Academy of Sciences. His current research interests include adaptive optics, wavefront sensing, image processing, and machine learning.

• • •